INDONESIAN JOURNAL ON GEOSCIENCE
Geological Agency
Ministry of Energy and Mineral Resources

Journal homepage: http://ijog.geologi.esdm.go.id
ISSN 2355-9314, e-ISSN 2355-9306

Wireline Log Responses, Mudweight, Clay Mineralogy, and Implied Overpressure Condition: Insights from Aru Field, North Sumatra Basin

Mohammad Syaiful[1], Lambok M. Hutasoit[2], Agus M. Ramdhan[2], and Agus Haris Widayat[3]

[1]Department of Geology, Institut Teknologi Bandung
Jln. Ganesha No. 10, Bandung 40132, West Java, Indonesia
[2]Department of Geology and Department of Groundwater Engineering, Institut Teknologi Bandung
Jln. Ganesha No. 10, Bandung 40132, West Java, Indonesia
[3]Department of Mining Engineering, Institut Teknologi Bandung
Jln. Ganesha No. 10, Bandung 40132, West Java, Indonesia

Corresponding author: mohammadsyaiful@gmail.com
Manuscript received: June, 13, 2019; revised: January, 9, 2020;
approved: January, 20, 2020; available online: April, 30, 2020

Abstract - This paper comprehensively discusses overpressuring in the North Sumatra Basin by using wireline log, drilling events and parameters, and clay mineralogical data. It shows an interesting phenomenon related to overpressuring in this basin, *i.e.* strong log reversals indicating high overpressure, yet the mudweight used during drilling was relatively low, indicating low overpressure with no significant drilling events noted in the final well report.The result of the study shows that wireline log is the best parameter to imply overpressure magnitude. Regarding low mudweight in the strong log reversal zone, it would be elucidated that the drilling in that zone was in underbalance condition with respect to shale pressure, but not to sandstone pressure. The sandstone pressure is interpreted to be lower than shale pressure due to lateral drainage process. By applying the Eaton's method, the estimated maximum overpressure magnitude in the Baong Formation is in the range of 1,594 - 3,185 psi. or equivalent to the mudweight of 1.61 - 192 g/cm^3. The analysis of wireline log in combination with clay mineralogical data shows that there are two compaction lines in the studied area, *i.e*. smectitic and illitic compaction lines. The cross-plot of density and sonic logs in shale section suggest that the cause of overpressure was loading mechanism. The scanning electron microscope (SEM) image confirms that in overpressure zone, grain to grain contact is still able to be observed fairly well, inferring that loading mechanism is really the cause of overpressure in the studied area.

Keywords: North Sumatra Basin, overpressure, underbalance, loading, smectite and illite compaction

How to cite this article:
Syaiful, M., Hutasoit, L.M., Ramdhan, A.M., and Widayat, A.H., 2020. Wireline Log Responses, Mudweight, Clay Mineralogy, and Implied Overpressure Condition: Insights from Aru Field, North Sumatra Basin. *Indonesian Journal on Geoscience*, 7 (2), p.105-119. DOI: 10.17014/ijog.7.2.105-119

Introduction

The North Sumatra Basin has long been recognized as an overpressured basin. Aziz and Bolt (1984) identified the presence of overpressure in the Aru Field, and the top of overpressure is mostly located in a massive shale sequence of the post rift deposit of Lower Keutapang Formation. They showed the occurrence of shale diapir as an evidence of high overpressure condition, and identified pressure regression into the Arun Limestone located below the highly overpressured Baong Formation. Ramdhan *et al.* (2018) recognized the regression as the evidence of active lateral reservoir drainage in the area. Hutasoit *et al.* (2013) investigated overpressure characteristics in the Aru Field,

North Sumatra Basin, and they obsserved that there were two overpressure conditions in the Baong Formation, *i.e.* mild overpressure in the Upper Baong and high overpressure in the Lower Baong. They also identified a shoulder effect in shale velocity surrounding Mid-Baong Sand, thus pressure regression, indicating that the sand was actively drained laterally. In several wells in the North Sumatra Basin, related to overpressure, this study found an interesting phenomenon, *i.e.* strong sonic and resistivity reversals into high sonic and low resistivity values, respectively. It indicated a high overpressure magnitude, yet the mudweight used during drilling was low without any significant problems showing a low overpressure magnitude (Figure 1). To explain this phenomenon, Syaiful *et al*. (2014) proposed that shales in the shallow, hydrostatically pressured section had experienced shallow compaction due to carbonate cementation. The sediments in that section might be less compacted in the past and the overpressure data points might not be too high from the 'past compaction line', and they would fit the low mudweight, indicating low overpressure.

Clay minerals are also analyzed in combination with the understanding of geological condition of the area and industrial best practice, in order to know whether this hypothesis is sufficient to explain the mismatch of log responses *vs*. the mudweight. This research has assigned some insights of overpressuring in the area. It suggested that the low mudweight was applied during drilling in order to avoid loss circulation in the sandstone section (keeping close to balance or only slight overbalance with respect to sandstone pressure), while the shales located above and below the sandstone unit were in a high overpressure condition, and therefore, the drilling was underbalance with respect to shale pressure. The lateral reservoir drainage was also the responsible process for this pressure regression. This research has offered a better understanding on shale compaction and overpressure generating mechanism in the studied area.

The discussion in this paper starts by examining the research problem and the hypothesis to prove. The methodology used in this study is then described, followed by the analysis of wireline, mudweight, clay mineralogy, and pressure data. Several interesting points are given in this study then discussed.

Geology

The studied area is located in the Aru Field, North Sumatra Basin (Figure 2). The basin is composed of Tertiary sedimentary rocks depos-

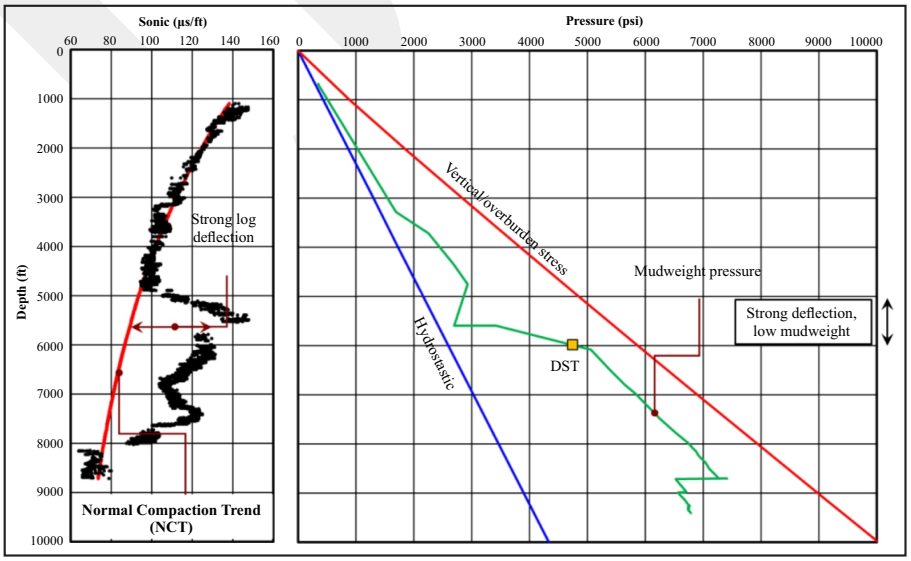

Figure 1. Mismatch between log response and mudweight used during drilling in the studied area (taken from PPA-1 well).

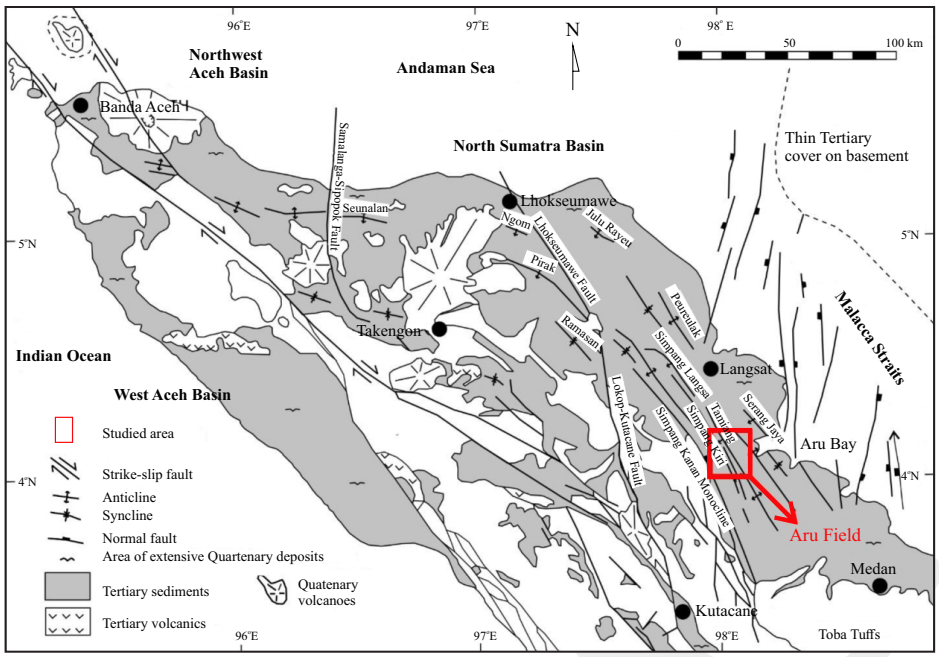

Figure 2. Studied area (redrawn from Barber and Crow, 2005).

ited above Pre-Tertiary basement (*e.g.* Davies, 1984). The basin was formed as a consequence of regional extensional tectonic experienced by South East Asia region in Eocene (Hall, 2012). The north-south horsts and grabens series were formed as a result of the extension. The basin has also experienced several episodes of inversion causing the development of anticlines, strike-slip movement of faults, and outcropping of rock formations (Barber and Crow, 2005).

The generalized stratigraphic column of the North Sumatra Basin is shown in Figure 3. The basement of the basin is Carboniferous, Perm, and Triassic igneous and metamorphic rocks (Barber and Crow, 2005). The oldest sedimentary rock is Tampur Formation, marking the pre-rift period in the basin (Eocene-Oligocene). This formation is dominated by limestone with some chert and basal conglomerate interbeds. Overlying unconformably the Tampur Formation is the syn-rift sequence of Parapat, Bampo, and Belumai Formations. The Parapat Formation is dominated by poorly sorted sandstone, breccia, conglomerate, and shale (Mulhadiono and Sutomo, 1984). The Bampo Formation is dominated by thick shale, while the Belumai Formation is composed of clastic limestone, shale, and sandstone.

Above the syn-rift sequence, reefal limestone of Peutu Formation was built in basinal highs, while in the basinal deep, a thick sequence of shale of Baong Formation was deposited. Several companies working in the North Sumatra Basin gave different names for the reefal limestone, according to its geographical location. For example, Exxon Mobil named it Arun Limestone in Aru Field, and Medco named it as Alur Siwah Limestone in Alur Siwah Field. The deposition of Baong Formation marks the maximum transgression experienced by the basin. Within the Baong Formation, turbiditic sandstones were deposited (Cameron *et al.*, 1980).

The basin experienced a major inversion during Miocene-Pleistocene. The western part of the basin was uplifted, providing sediment supply for the basinal area. The syn-inversion sedimentation has resulted in Keutapang, Seurula, and Julurayeu Formations. The formations comprise sandstone, mudrocks, tuff, and lignite in some places. During Quaternary, the basin experienced inversion again, causing almost all formations to outcrop on the surface. The inversion was followed by erosion and sedimentation in some places, and it has resulted in sedimentary terraces in several places.

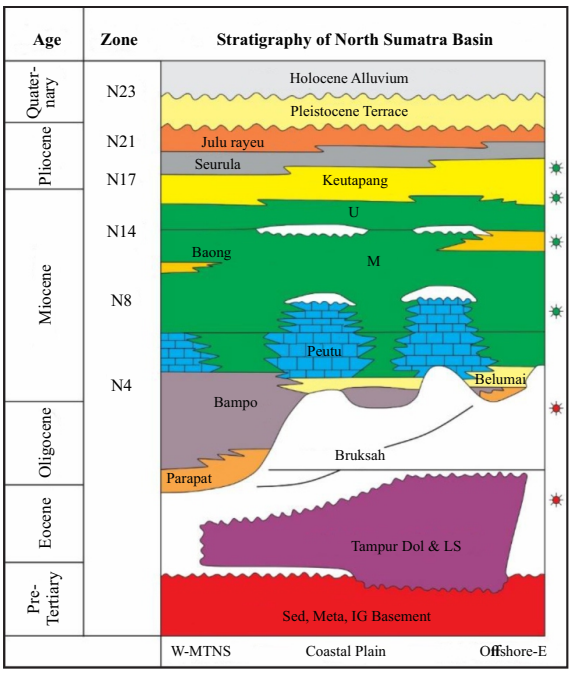

Figure 3. Stratigraphic column of the North Sumatra Basin (redrawn and simplified from Pertamina BPPKA, 1996).

Methodology

Wireline Log, Drilling Parameters, and Events

The wireline logs in shale section have long been used to analyze overpressure and compaction of shale (*e.g.* Ramdhan and Goulty, 2011). In normally compacted sediments, the density and resistivity log values will increase with increasing depth, while the sonic log values will decrease with increasing depth. If overpressure occurs, starting at the top of overpressure, the resistivity and sonic logs will stop to increase and decrease, respectively. In this case, the overpressure was caused by loading mechanism, the density log would also stop in increasing. If the overpressure was caused by fluid expansion mechanism, then the density log would continue to increase, irrespective of the presence of overpressure (Bowers, 1995).The overpressure generating mechanism can also be analyzed from density and sonic cross-plot in shale section (Figure 4). Sargent *et al*. (2015) stated that if overpressure was caused by loading mechanism, then the overpressure points would cluster on normal compaction lines, either in smectitic or illitic line. If overpressure was generated by fluid expansion mechanism, then the overpressure points will be off the compaction trends, and they will be located along the arc.

The method of overpressure estimation in shale section also uses wireline log as the main input, *e.g*. Eaton's method (Eaton, 1975). The Eaton's method uses sonic, resistivity, and d'exponent (normalized drilling rate) as the main input. The schematic of the Eaton's method is shown in Figure 5. The greater the data are deflected from the normal compaction trend (NCT), the greater the overpressure magnitude. The NCT is constructed by interpolating the normally pressured section data, subsequently it is extrapolated into overpressure section. The equation of the Eaton's method for the sonic log is:

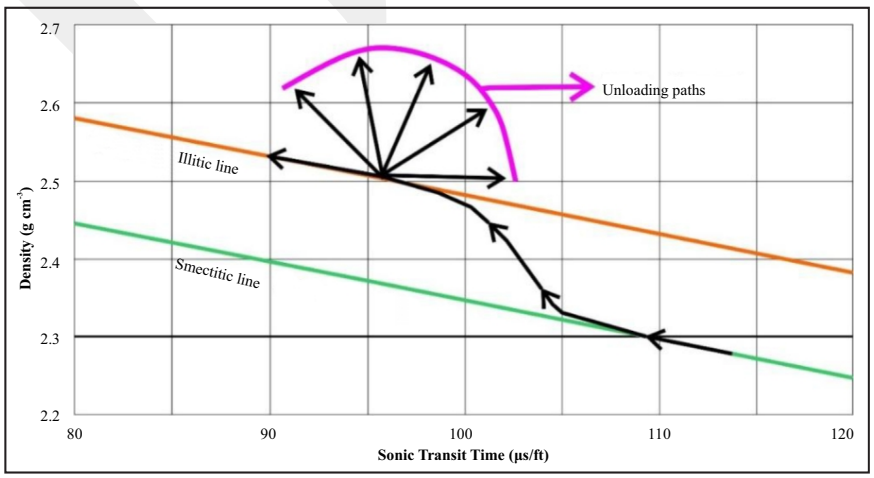

Figure 4. Sonic and density cross-plot to identify overpressure generating mechanism (redrawn from Sargent *et al.,* 2015). In this paper, fluid expansion is used, instead of unloading.

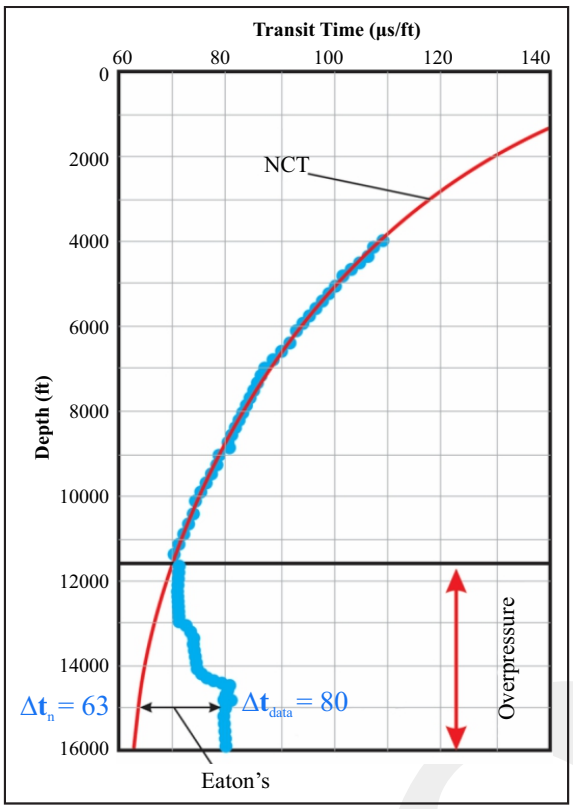

Figure 5. Schematic of Eaton's method.

$$P = \sigma_v - (\sigma_v - P_n)\left(\frac{\Delta t_n}{\Delta t_{data}}\right)^3 \quad \text{.....(1)}$$

where:

P = pore pressure (ML-1T-1)

σv = vertical/overburden stress ($ML^{-1}T^{-1}$)

Δt_{data} = sonic log (TL^{-1})

The subscript n indicates the value of the parameters on the NCT.

Eaton (1975) compared the estimated shale pore pressure obtained from Equation (1) with measured pore pressure in reservoir (mostly sandstone) sections. The majority of the measured data fit for the exponent of 3 in the equation. Eaton (1975) also tried several exponents prior to coming up with the exponent of 3. This process is known as calibration process.

In the case of the measured pore pressure is limited, drilling parameters and events are usually used to calibrate the estimated shale pore pressure. Among the parameters and events are kicks, increase in gas content in drilling hole, loss circulation, cavings, and mudweight used during drilling. Kicks are influx of fluid from relatively high permeable formation into a bore hole, because the bore-hole pressure (borne by mudweight) is less than the formation pressure, and it is said as underbalance. In drilling, the kicks are handled by increasing the mudweight so that the bore-hole pressure can be maintained to be higher than formation pressure. The formation pressure is therefore estimated to be between mudpressure, prior and after the kicks. The increase in gas content is similar with kicks, except that the drilling encounters less permeable units (*e.g.* shales).

Loss circulation is an event when drilling mud enters the formation, so that it cannot be circulated back into the surface. Loss circulation can be categorized into two, *i.e.* natural loss and induced loss. The natural loss usually occurs when drilling penetrates a hydrostatically pressured - high permeable formation, and the mudweight pressure is significantly higher than the formation pressure (termed as overbalance), but still below fracture pressure. The induced loss happens when the mudweight pressure reaches the fracture pressure, so that it will initiate hydro-fracturing, causing the mud enters the fractured formation. Therefore, the mud pressure can be used as a proxy of maximum likely pressure in formation in the case of the presence of loss.

Cavings are material resulted from hole enlargement. The hole enlargement could be caused by pore pressure and/or mechanical instability caused by certain in-situ stress states. Theoretically, severe underbalance drilling will trigger tensile failure, causing hole enlargement, producing splintery cavings. Meanwhile, stress instability will trigger shear failure, causing hole enlargement, and producing blocky cavings.

Traditionally, the mud pressure, in the absence of major drilling events as mentioned above, is usually interpreted as a maximum likely pressure in formation. Unlike the above drilling events, the mudweight data are always available. In this study, this traditional view of the mudweight as proxy for pore pressure is analyzed and discussed.

Clay Mineralogy

As mentioned previously, the crossplot of wireline log data can be used to imply compaction state of the shales, whether it is in early compaction stage (eo-diagenesis/smectitic compaction line) or late compaction stage (telo-diagenesis/illitic compaction line) (Figure 4). In this study, the crossplot is used for clay mineralogical analysis in usage of X-ray diffraction (XRD) and scanning electron microscope (SEM). The data sources for the analysis are cutting samples taken systematically from near surface down to the total depth (TD) of wells. By performing semiquantitative XRD analysis, the clay mineral composition through depth can be observed. Meanwhile, from SEM analysis, the presence or absence of mechanical compaction through depth can be analyzed, indicated by the presence or absence of grain to grain contact.

Wireline, Mudweight, Clay Mineralogy, and Pore Pressure Data Processing

Two typical overpressured wells chosen are discussed in this paper, *i.e.* PPA-1 and TPB-1. Both wells are located in the basinal deep (graben).

PPA-1

Stratigraphic formations, pressure-depth (P-D) plot, and wireline log in shale section in this well are shown in Figure 6. This well penetrates Pliocene sediments of the Seurula Formation down tosyn-rift section of the Belumai Formation. P-D plot shows there is one DST point at the depth of 6,000 ft. in the Mid-Baong Sand, showing the pressure value of 4,741 psi. The DST point at the Mid-Baong Sand shows a relatively high pressure value, equivalent with 15.4 ppg of mudweight. The mudweight was started to increase significantly above hydrostatic gradient starting at the depth of ~3,200 ft. However, density, sonic, and resistivity logs started to reverse, indicating the first appearance of overpressure (top of overpressure) (see methodology), at the depth of ~5,000 ft. Therefore, the increase in mudweight below 5,000 ft. does not reflect overpressure. It is interesting that in the depth interval of ~5,000 - 6,000 ft., the mudweight is not so high, yet the reversal in logs is strong. This circumstance will be discussed in the discussion section.

The result of semiquantitative XRD in this well is given in Table 1 and Figure 7. From the bulk composition, it can be seen that carbonate mineral is a minor constituent. Kaolinite is the dominant mineral in the entire section. It is interesting that from the depth of 1,960 m (~6,429 ft.) discrete smectite has disappeared. The crossplot of density *vs*. sonic in shale section in this well is shown in Figure 8. It can be seen that the disappearance of discrete smectite is in agreement

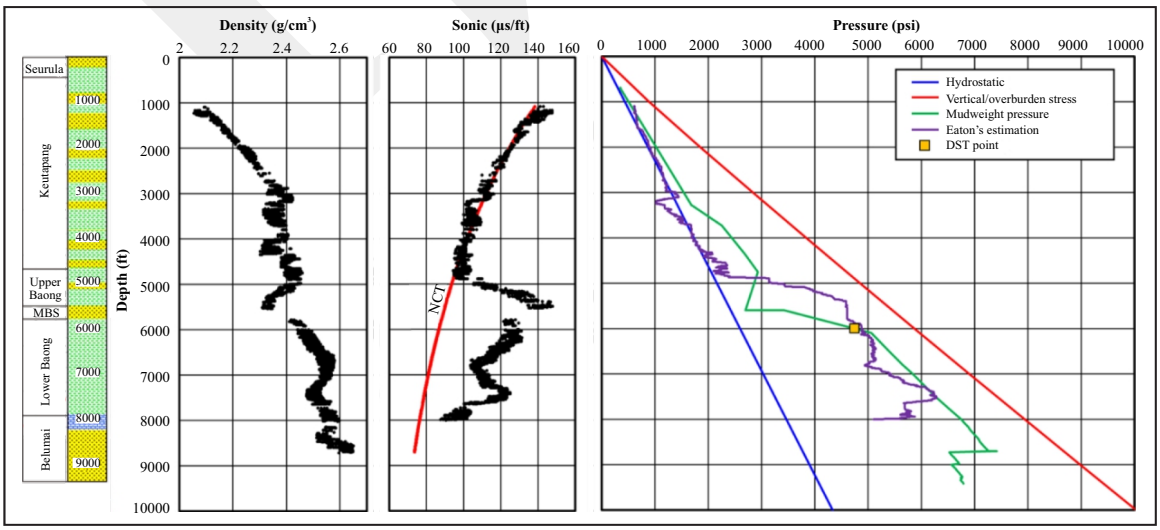

Figure 6. Stratigraphic formation, P-D plot, and wireline log in shale section of PPA-1.

Table 1. Semiquantitative XRD of PPA-1 (%-weight value)

Depth (m)	Clay					Carbonate			Other				Total		
	Smectite	Mixlayer Illite Smectite	Illite	Kaolinite	Chlorite	Calcite	Dolomite	Siderite	Quartz	K-feldspar	Plagioclase	Gypsum	Clay	Carbonate	Other
700	16	9	5	31	6	2	tr	tr	9	10	10	2	67	2	31
800	13	7	13	15	4	2	tr	tr	29	7	6	4	52	2	46
900	14	10	11	18	5	2	tr	tr	24	6	6	4	58	2	40
1000	16	16	7	12	5	6	2	tr	15	9	9	3	56	8	36
1102	7	8	16	9	3	1	2	1	34	9	7	3	43	4	53
1200	13	8	12	12	3	2	1	tr	25	12	9	3	48	3	49
1300	12	7	15	8	2	2	1	tr	37	5	5	6	44	3	53
1400	10	9	13	10	3	4	1	tr	26	13	9	2	45	5	50
1500	13	8	14	10	3	8	tr	tr	30	5	6	3	48	8	44
1629	7	9	8	18	3	2	1	tr	16	20	14	2	45	3	52
1750	7	11	8	25	6	2	2	tr	12	13	11	3	57	4	39
1850	8	10	5	23	5	2	2	tr	9	20	16	tr	51	4	45
1960	0	10	12	8	4	4	2	tr	24	15	12	9	34	6	60
2000	0	8	5	33	5	3	2	tr	9	19	16	tr	51	5	44
2100	0	9	7	27	4	2	2	tr	9	22	17	1	47	4	49
2250	0	9	12	24	5	2	2	tr	26	7	9	4	50	4	46
2300	0	0	12	18	4	23	2	tr	25	6	8	2	34	25	41
2498	0	4	21	2	2	13	1	tr	37	9	9	2	29	14	57
2600	0	7	20	8	2	2	1	tr	42	9	7	2	37	3	60
2700	0	0	20	5	2	2	1	tr	44	12	10	4	27	3	70
2798	0	0	10	26	0	9	3	tr	18	18	15	1	36	12	53

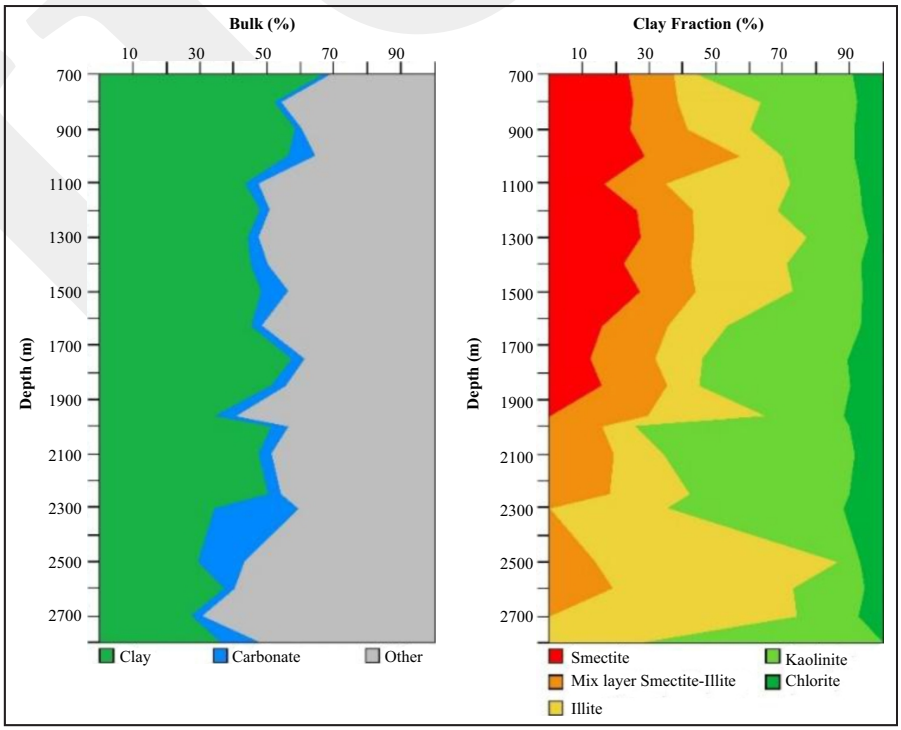

Figure 7. Semiquantitative XRD of PPA-1.

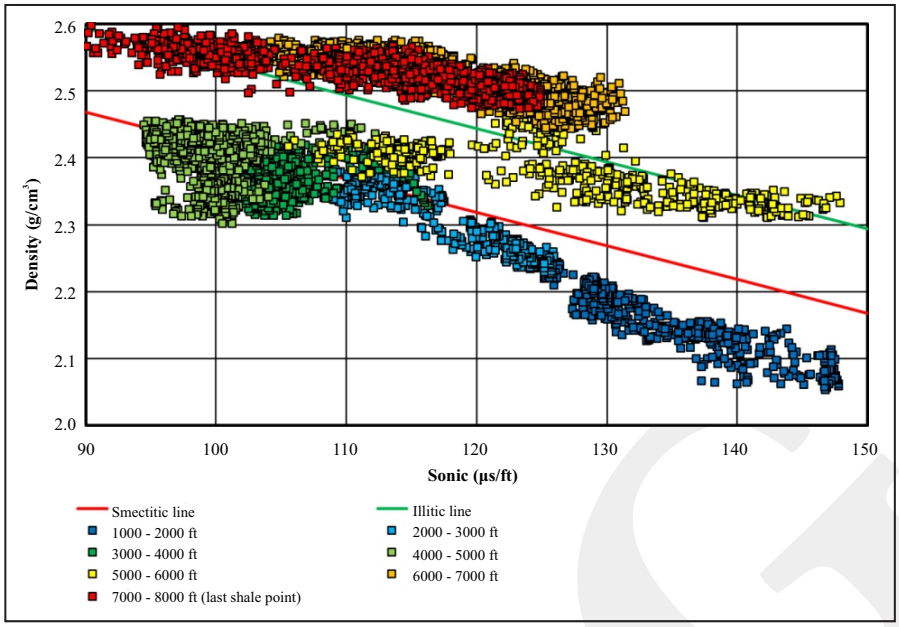

Figure 8. Density-sonic cross plot in shale section of PPA-1.

with shifting in compaction line from smectitic line into illitic line.

An SEM photomicrograph in hydrostatically pressured, smectitic zone, at the depth of 1,200 m (3,936 ft.) is shown in Figure 9a.The kaolinite can be observed very well, marked by ragged edge and book structure. The quartz grain can also be observed from its hexagonal crystal feature. Grain to grain contact can be fairly well observed, indicating the effective stress.Thus, mechanical compaction is still the controlling factor for shale compaction in the hydrostatic - smectitic zone.

An SEM photomicrograph in overpressured, illitic zone, at the depth of 2,498 m (~8,193 ft.), is shown in Figure 9b. The illite can very well be observed, marked by flatty structure. It is interesting that grain to grain contact still can fairly well be recognized, also indicating that mechanical compaction is still the controlling factor for shale compaction in the overpressured- illitic zone.

TPB-1

Stratigraphic formations, pressure-depth (P-D) plot, and wireline log in shale section in this well are shown in Figure 10. This well also pen-

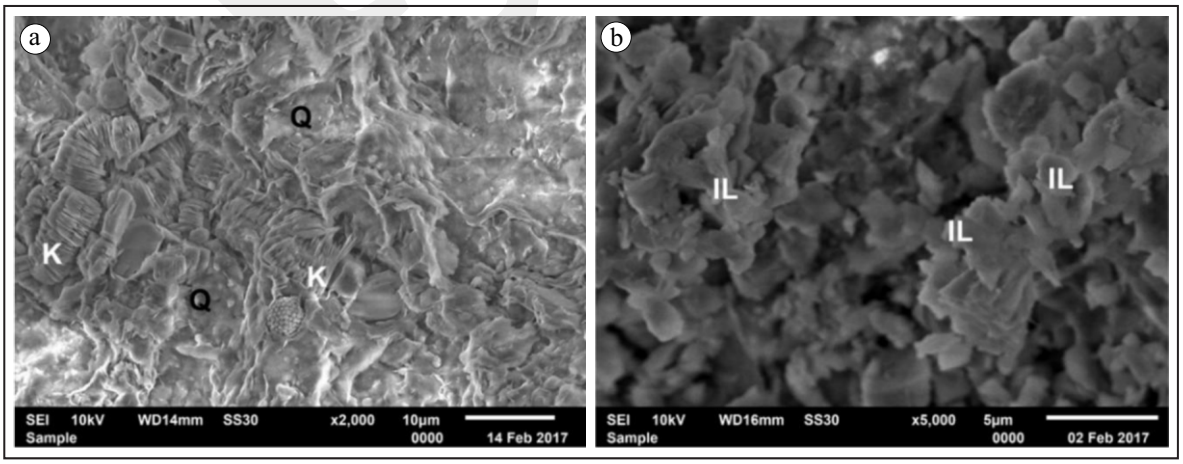

Figure 9. SEM microphotographs in PPA-1; (a) 1200 m, hydrostatic (b) 2498 m, overpressure.

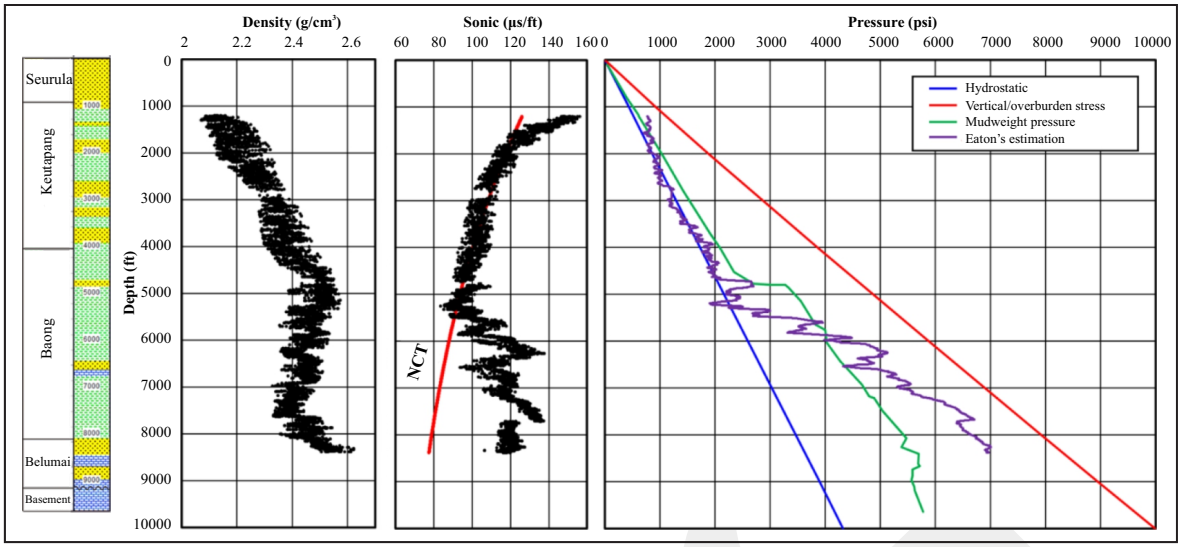

Figure 10. Stratigraphic formation, P-D plot, and wireline log in shale section of TPB-1.

etrated Pliocene sediments of the Seurula Formation down to syn-rift section of the Belumai Formation. Direct pressure data are not available in this well. The mudweight commences to increase significantly above hydrostatic gradient starting at the depth of ~4,800 ft. However, density, sonic, and resistivity logs begin to reverse, indicating the first appearance of overpressure (top of overpressure) (see methodology), at the depth of ~5,200 ft. Therefore, the increase in mudweight below 5,200 ft. does not reflect overpressure. Compared with PPA-1, mudweight in overpressure section, in the interval of 5,200-TD (9,500 ft.), is lighter, yet the log reversal magnitudes in both wells are relatively similar. This circumstance will also be discussed in the discussion section.

Result of semiquantitative XRD in this well is given in Table 2 and Figure 11. From the bulk composition, it can be seen that carbonate minerals are minor constituent. Kaolinite is the dominant mineral in the entire section. It is interesting that starting at the depth of 2,000 m (6,560 ft.) discrete smectite has disappeared. The crossplot of density-sonic in shale section in this well is shown in Figure 12. It can be seen that the disappearance of discrete smectite is in agreement with shifting in compaction line from smectitic line into illitic line.

An SEM photomicrograph in hydrostatically pressured, smectitic zone, at the depth of 300 m (984 ft.), is shown in Figure 13a. Smectite can very well be detected, marked by webby-beehive structure. Grain to grain contact can fairly well be recognized indicating that effective stress.Thus, mechanical compaction is still the controlling factor for shale compaction in the hydrostatic-smectitic zone.

An SEM photomicrograph in overpressured, illitic zone, at the depth of 2,250 m (~7,380 ft.), is shown in Figure 13b. Illite can very well be detected, marked by flatty structures. It is interesting that grain to grain contact still can fairly well be observed, also indicating that mechanical compaction is still the controlling factor for shale compaction in the overpressured - illitic zone.

Analysis and Discussions

Overpressure Magnitude *vs.* Mudweight

As mentioned in Introduction, Syaiful *et al.* (2014) proposed a shifting in compaction line within a shallow section due to carbonate cement in explaining the mismatch between log response showing high reversal indicating overpressure with low mudweight indicating low overpressure. However, result of the clay mineralogical analysis shows that the carbonate minerals are minor constituents in both wells analyzed in this study. Therefore,the shifting is ruled out

Table 2.Semiquantitative XRD of TPB-1(%-weight value)

Depth (m)	Clay					Carbonate			Other				Total		
	Smectite	Mixlayer Illite Smectite	Illite	Kaolinite	Chlorite	Calcite	Dolomite	Siderite	Quartz	K-feldspar	Plagioclase	Gypsum	Clay	Carbonate	Other
100	19	9	9	17	5	1	1	2	20	6	7	4	59	4	37
200	15	9	10	18	4	1	1	2	22	7	7	4	56	4	40
300	9	3	20	5	2	1	1	2	42	6	7	2	39	4	57
400	23	10	5	24	5	2	2	2	10	7	8	2	67	6	27
500	25	8	7	17	6	2	2	2	15	7	7	2	63	6	31
600	23	9	7	16	5	2	2	2	16	9	7	2	60	6	34
690	14	10	12	10	3	1	1	2	28	7	7	5	49	4	47
800	35	11	5	15	7	1	1	1	10	6	6	2	73	3	24
900	23	10	7	22	6	1	1	1	12	8	6	3	68	3	29
1000	21	9	8	14	5	2	2	2	17	8	8	4	57	6	37
1100	20	9	8	19	6	1	1	2	16	7	7	4	62	4	34
1200	19	9	8	18	6	tr	1	2	18	8	8	3	60	3	37
1300	24	11	6	20	6	tr	tr	1	13	8	7	4	67	1	32
1476	8	10	7	22	3	1	1	3	15	16	12	2	50	5	45
1600	12	9	7	25	5	2	1	2	15	10	9	3	58	5	37
1676	13	10	5	27	5	4	2	2	10	11	9	2	60	8	32
1800	11	7	10	23	5	tr	1	2	20	8	8	5	56	3	41
1900	22	17	3	23	7	1	1	4	5	8	7	2	72	6	22
2000	18	22	5	7	5	2	2	4	13	10	8	4	57	8	35
2124	0	9	11	17	4	tr	2	3	22	19	14	3	39	4	57
2250	0	11	6	34	5	2	2	2	11	13	13	3	55	5	40
2326	0	9	10	25	4	tr	2	3	18	17	14	3	46	4	50
2401	0	10	6	34	6	2	2	3	10	14	13	2	55	6	39
2552	0	10	8	24	5	10	tr	2	16	14	11	3	46	11	43
2600	0	8	9	26	4	12	tr	2	18	8	9	4	47	14	39
2700	0	7	6	10	3	40	2	2	15	5	8	3	26	44	30
2798	0	13	8	9	4	2	2	3	15	28	19	2	32	6	62

in compaction line as the possible cause of the mismatch.

Theoretically, the deflection in the wireline logs as discussed above is proportional to overpressure magnitude, *i.e.* the higher the deflection, the higher the overpressure magnitude. However, in PPA-1, in the interval of ~5,000 - 6,000 ft., the presence of high overpressure is not reflected by higher mud-weight used during drilling. As drilling penetrated a permeable unit, no kicks were observed in the well. Also, there was no hole enlargement detected as indicated by the absence of caving. Traditionally, with the absence of major drilling events as described above, the mudweight is commonly interpreted as the maximum likely formation pressure. Therefore, the formation pressure as interpreted from wireline logs is in conflict with the formation pressure as interpreted from mudweight data.

A similar conflicting condition occured when wire line log responses were compared in PPA-1 and TPB-1 (see Figures 6 and 10). At the depth of ~7,000 ft., sonic logs in PPA-1 and TPIB-1 show the same magnitude of deflection, *i.e.* ~ 28 μs/ft. Yet, the mudweight in that depth differs significantly, *i.e.* 1.92 g/cm^3 in PPA-1 and 1.55 g/cm^3 in TPB-1, corresponding to the overpressure magnitude of 2,813 psi. and 1,686 psi. in PPA-1 and TPB-1, respectively. Both wells did not experience significant drilling problems applying those mudweight.

In PPA-1, as mentioned above, there is one pressure measurement point (DST) in sand-

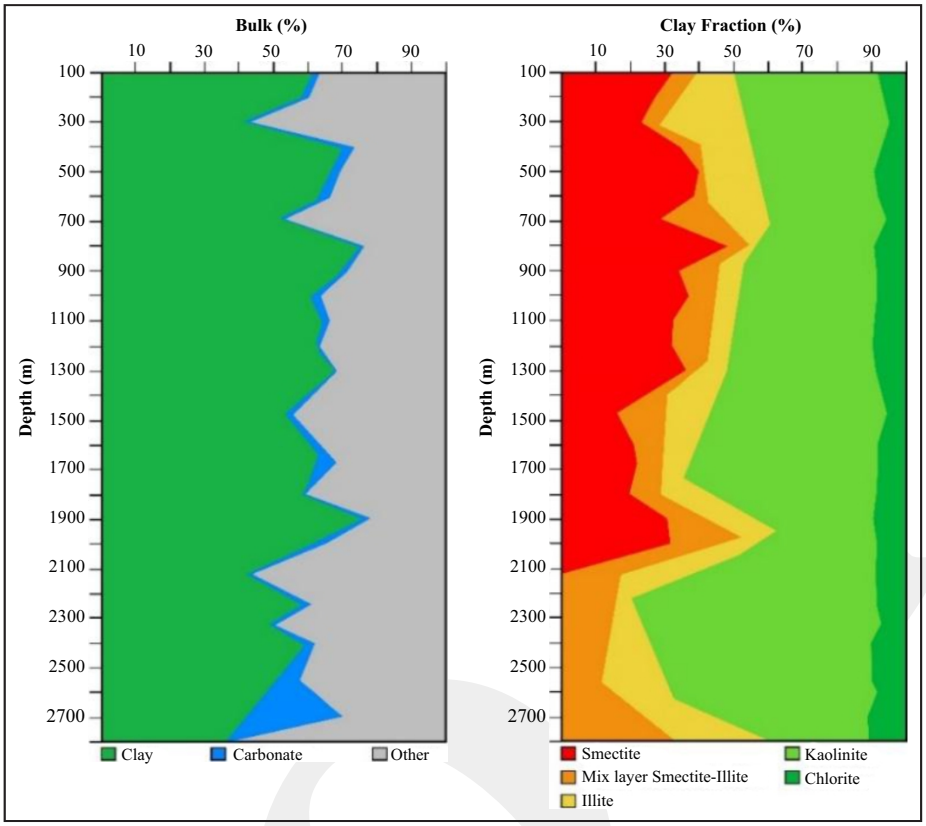

Figure 11. Semiquantitative XRD of TPB-1.

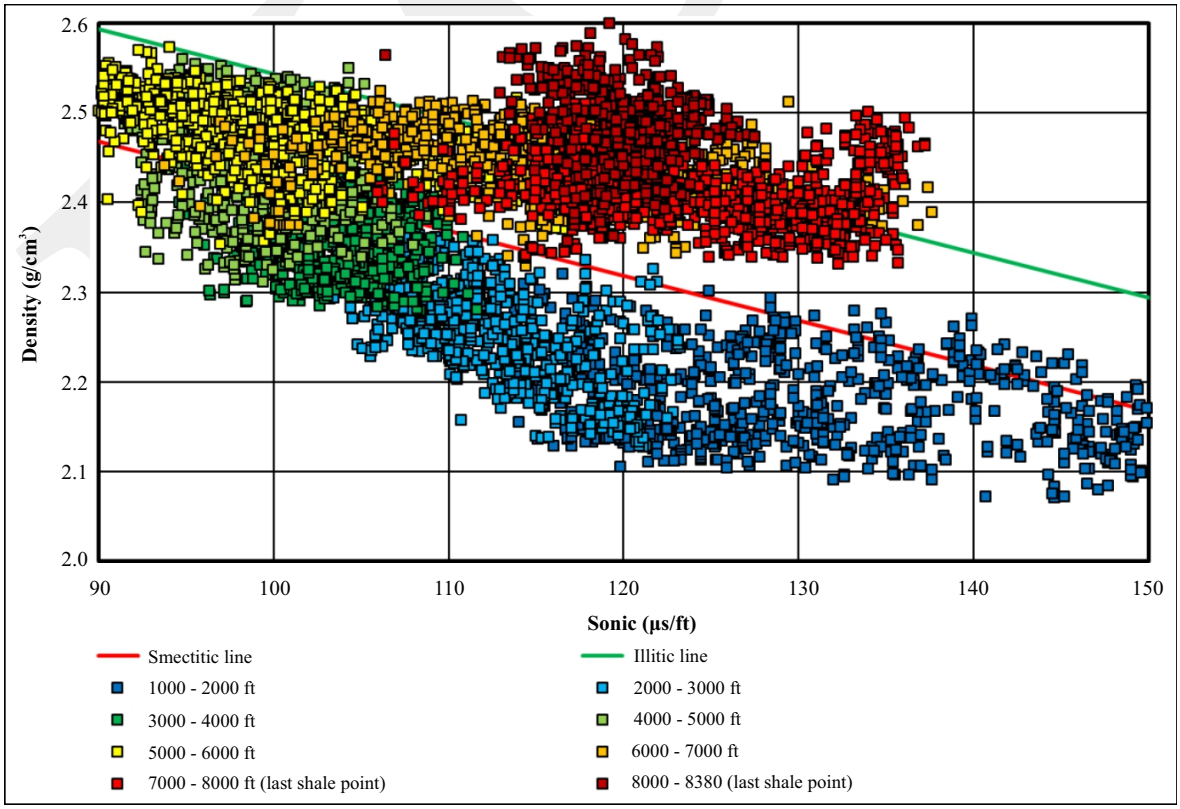

Figure 12. Density-sonic cross plot in shale section of TPB-1.

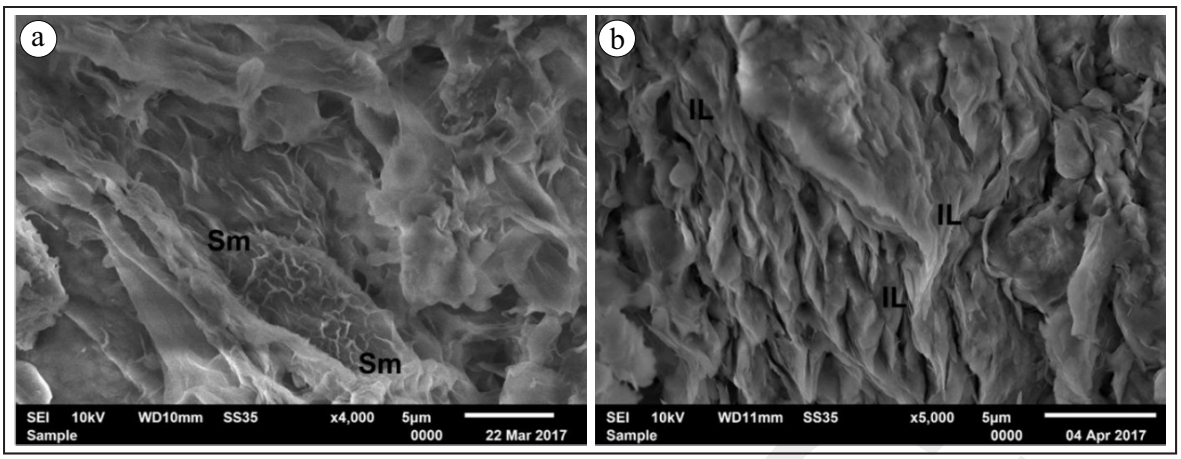

Figure 13. SEM photomicrographs in TPB-1; (a) 300 m, hydrostatic, (b) 2250 m, overpressure.

stone at the depth of ~6,000 ft.with the value of 4,741 psi. (Figure 6). It can be seen that the DST pressure is as high as mudweight pressure. It is interpreted that at least this pressure reflects shale pressure, because the overpressure magnitude is very high. By using this point as a calibration point, then the overpressure was tried to be estimated in shale section by applying the Eaton's method (Equation1) for sonic log. The result of the estimation using Eaton's method in PPA-1 is also shown in Figure 6. The Eaton's exponent used in that figure is 3. It can be seen, that the Eaton's method can match the measured pore pressure at the depth of ~6,000 ft. The implication of the result of the method is that the depth interval of 5,000 - 6,000 m was drilled in a severe underbalance condition with respect to shale pressure. Meanwhile, the depth interval of ~6,000 - 8,000 ft. was drilled in a slight overbalance condition with respect to shale pressure. In TPB-1, the measured pore pressure was not available. Similar approach as for PPA-1 to estimate shale pore pressure in TPB-1 was applied. The assumption is that since the generating mechanism is similar (see discussion on overpressure generating mechanism below), then the same method should be applicable. Moreover, the geological condition in both wells is similar, and its distance is relatively short. The result of shale pore pressure estimation is shown in Figure 14. In the depth interval of ~5,000 - 6,000 ft., the drilling was in overbalance condition, while starting at the depth of ~6,000 - 8,500 ft., the drilling was in underbalance condition.

Comparing the shale pressure estimation in both wells, the Eaton's estimation results are consistent pressure pattern in both wells, *i.e.* hydrostatic, transition zone into high overpressure and high overpressure zone (Figure 14). The Eaton's method also resulted in consistent overpressure magnitude with respect to the magnitude of sonic deflection. For example, at the depth of 7,000 ft., as mentioned above, there is sonic deflection in both wells of about 28 µs/ft. By applying the Eaton's method, the deflection resulted in estimated overpressure of 2,370 psi. in both wells.

It is interesting to observe that there is underbalance section in the depth interval of 5,000 - 6,000 ft. in PPA-1 and in the interval of 6,000 - 8,500 ft. in TPB-1, yet there is no information about the presence of kicks and cavings. In PPA-1, there are several sandstone layers in the underbalance interval, and stratigraphically they belong to turbiditic sandstone of the Baong Formation. The absence of kick in these sandstones could be explained by lateral reservoir drainage process. Sandstone experiencing lateral reservoir drainage will possess pore pressure lower than its surrounding shale. Ramdhan *et al*. (2018) showed that turbiditic sandstone of Baong Formation has been experiencing a lateral reservoir drainage. The outcropping of this sandstone due to basin inversion process is the cause of this lateral drainage process. Therefore, the drilling in the interval

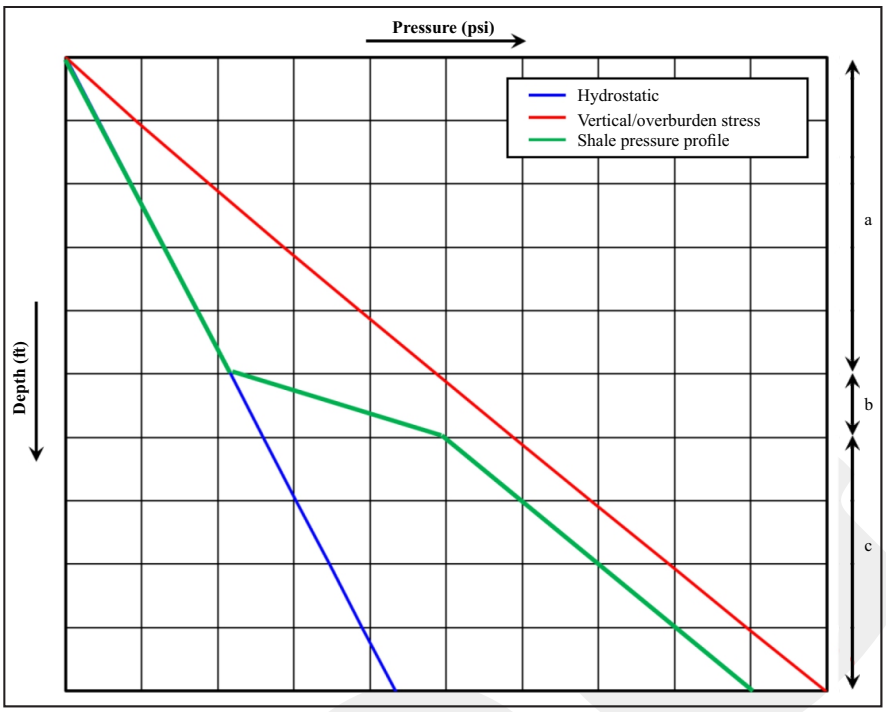

Figure 14. Schematic of shale pressure profile in the studied area. (a) hydrostatic, (b) transition, (c) high overpressure.

of 6,00 - 8,500 ft. is indeed in an underbalance condition with respect to shale pressure, but it is close to balance or even slightly overbalance with respect to sandstone pressure. Meanwhile in TPB-1, the underbalance interval is located in thick shale sequence of the Baong Formation with no high permeable unit. Therefore, the absence of kick in underbalance section in TBP-1 could be explained by this circumstance.

In the final well report, the information of the presence or absence of cavings within the underbalance interval in PPA-1 and in TPB-1 is not available. Based on personal communication (colleagues in an oil industry), cavings will be stated in the final well report if they cause major drilling problems such as hole pack-off. If they are present but they can still be circulated to the surface, they are usually not reported. The best way to analyze the presence of cavings is to read daily drilling report. However, the authors do not have such access to the report. Another possibility of the absence of caving in underbalance drilling is caused by the nature of this event. To date, it is still unclear whether the caving is a sudden process or time-dependent process. If the case is the latter, then a high penetration rate may avoid cavings to be present.

As mentioned in the methodology, traditionally, in the absence of major drilling events, mudweight pressure is usually interpreted as maximum likely pore pressure. In this paper, the presence of lateral reservoir drainage and some uncertainties in the nature of cavings has been demonstrated, without additional information which should be treated skeptically as proxy for pore pressure, both in sandstone and shale sections.Taking the depth interval of ~6,000 - 8,000 ft. as a maximum overpressure in Baong Formation (see Figures 6 and 10), the magnitude of the maximum overpressure in this formation is in the range of 1,594 - 3,185 psi. of overpressure, or equivalent to the mudweight of 1.61 - 1.92 g/cm^3.

Shale Compaction and Overpressure Generating Mechanism

The clay mineralogical analysis as described above shows that the discrete smectite has disappeared at the depth of ~6,429 ft. in PPA-1 and ~6,560 ft. in TPB-1 (Figures 7 and 11). The

disappearance of the smectite correlates with the shifting in compaction line from smectitic line into illitic line as observed in density and sonic cross plot (Figures 8 and 12). It is therefore inferred that wireline log can be used to analyze a compaction state of the shale in the studied area. The equation of smectitic and illitic lines in the studied area as shown in Figures 8 and 12 are:

Smectitic: $\rho = 2.918 - 0.005\Delta t$ .....(2)

Illitic: $\rho = 3.044 - 0.005\Delta t$ .....(3)

The crossplots in Figures 8 and 12 also show that overpressure points are still located on the compaction line, *i.e.* on the illitic line, and it is very indicative of overpressure that is generated by loading mechanism. The location of overpressure data points on the illitic line may lead to the interpretation that smectite to illite transformation may contribute to overpressure. However, there is no sign of the off compaction trend data. Moreover, the SEM images (Figures 9b and 13b) show that grain to grain contact (effective stress) can still be observed very well in the overpressure section. It means that mechanical compaction, thus loading overpressuring, is the main generating mechanism of overpressure. Therefore, in the studied area, smectite to illite transformation does not contribute to overpressure. It only shifts the normal compaction line without unloading the data. The small average percentage of smectite (11% in PPA-1 and 19% in TPB-1) may not be sufficient to cause fluid expansion overpressuring in the studied area.

Conclusions

Some points that can be concluded from this study are:

- The strong log reversal that does not correspond to high mudweight in the studied area is caused by underbalance drilling condition with respect to shale pressure. However, it may be close to balance or slight overbalance with respect to sandstone pressure. Lateral reservoir drainage is being responsible for such circumstance.
- The mudweight data without additional drilling event data should be treated skeptically for analyzing overpressure magnitude.
- The maximum overpressure in Baong Formation is in the range of 1,594 - 3,185 psi. of overpressure, or equivalent to the mudweight of 1.61 - 1.92 g/cm^3.
- The smectite to illite transformation could be observed both from clay mineralogical analysis and density-sonic cross plot in the studied area.
- Grain to grain contact indicating the presence of effective stress in the overpressure zone suggests that loading mechanism is still on going in that zone.
- The cause of overpressure in the studied area is loading mechanism as indicated by wireline log data and clay fabric image (grain to grain contact).

Acknowledgement

The authors thank Pertamina for data and sponsoring INOV (Indonesia Overpressure) research. M. Syaiful thanks Dr. Hermes Panggabean for clay mineralogy discussion, and Dr. Irwan Iskandar for permitting clay mineralogical analysis in Hydrogeology and Hydrochemistry Laboratory, Faculty of Mining and Petroleum Engineering, Institut Teknologi Bandung. Arifin drew some figures in this paper, and our sincere thank goes to him.

References

Aziz, A. and Bolt, L.H.,1984. Occurrence and detection of abnormal pressures from geological and drilling data, North Sumatra Basin. *Proceedings, 13th Indonesian Petroleum Association Annual Convention,* p.195-220, Jakarta. DOI: 10.29118/ipa.1191.195.220

Barber, A.J. and Crow, M.J., 2005. Structure and structural history. *In*: Barber, A.J., Crow, M.J.,

and Milsom, J.S. (eds.), *Sumatra: Geology, Resources, and Tectonic Evolution*, Geological Society of London Memoir No. 31. DOI: 10.1017/S0016756806212974

Bowers, G.L., 1995. Pore pressure estimation from velocity data: accounting for overpressure mechanisms besides under compaction. *SPE Drilling and Completion,* 10 (02), p.89-95. DOI: 10.2118/27488-PA

Cameron, N.R., Clarke, M.C.G., Aldiss, D.T., Aspden, J.A., and Djunuddin, A., 1980. The geological evolution of northern Sumatra. *Proceedings, 9th Indonesian Petroleum Association Annual Convention*, p.149-188.

Davies, P.R., 1984. Tertiary structural evolution and related hydrocarbon occurrences, North Sumatra Basin. *Proceedings, 13th Indonesian Petroleum Association Annual Convention*, p.19-49. DOI: 10.29118/ipa.2529.19.49

Eaton, B.A., 1975. The equation for geopressure prediction from well logs. *SPE*, 5544, 11pp.

Hall, R., 2012. Late Jurassic-Cenozoic reconstructions of the Indonesian region and the Indian Ocean. *Tectonophysics*, 570-571, p.1-41. DOI: 10.1016/j.tecto.2012.04.021

Hutasoit, L.M., Suseno, W., Siahaan, D., Ramdhan, A.M., Goulty, N., Syaiful, M., Bachtiar, A., Iskandar, I., Sadirsan, W., Arifin, M., Bahesti, F., and Endarmoyo, K., 2013. Overpressure characteristics in Pertamina's area in the North Sumatra Basin. *Proceedings, 37th Indonesian Petroleum Association Annual Convention and Exhibition*, p.101-117, Jakarta. DOI: 10.29118/ipa.0.13.g.153

Mulhadiono and Sutomo, J.A., 1984. The determination of economic basement of rock formation in exploring the Langkat - Medan area, North Sumatra Basin. *Proceedings, 14th Indonesian Petroleum Association Annual Convention*, p.75-107.

Pertamina BPPKA, 1996. *Petroleum Geology of Indonesia Basins: Principle, Methods and Application, V.1 North Sumatra Basin*. Pertamina BPPKA, Jakarta, 85pp.

Ramdhan, A.M. and Goulty, N.R., 2011. Overpressure and mudrock compaction in the Lower Kutai Basin, Indonesia: a radical reappraisal. *American Association of Petroleum Geologists, Bulletin*, 16, p.367-376. DOI: 10.1306/02221110094

Ramdhan, A.M., Hutasoit, L.M., and Slameto, E., 2018. Lateral reservoir drainage in some Indonesia's sedimentary basin and its implication to hydrodynamic trapping. *Indonesian Journal on Geosciences*, 5, p.65-80.

Sargent, C., Goulty, N.R., Cicchino, A.M.P., and Ramdhan, A.M., 2015. Budge-Fudge method of pore-pressure estimation from wireline logs with application to Cretaceous mudstones at Haltenbanken. *Petroleum Geoscience*, 21 (4), p.219-232. DOI: 10.1144/petgeo2014-088

Syaiful, M., Siahaan, D.G., Hutasoit, L.M., Ramdhan, A.M., Widayat, A.H., and Tribuana, I.Y., 2014. Shifting of compaction trend in the North Sumatra Basin and its implication to overpressure estimation in the North Sumatra Basin. *Proceedings, 38th Indonesian Petroleum Association Annual Convention*, IPA 14-G-358, Jakarta. DOI: 10.29118/ipa.0.14.g.358